An Effective Technique for Enhancing Anti-Interference Performance of Adaptive Virtual Antenna Array

[1]Wenxing Li, [1]Yipeng Li, [1]Lili Guo, and [2]Wenhua Yu

[1]College of Information and Communication Engineering
Harbin Engineering University, Harbin 150001, China

[2]Electromagnetic Communication Lab
The Pennsylvania State University, University Park, PA 16802

Abstract - In this paper**,** we proposed an effective technique to enhance the anti-interference performance of the adaptive antenna arrays. The null depth in the direction of interferers determines the anti-interference performance of an adaptive antenna array. However, the null depth generated by the conventional **v**irtual **a**rray **t**ransformation (VAT) algorithm is usually not sufficient. By introducing the interference direction information into the transformation matrix, we can effectively improve the level of null depth; in turn, the **an**ti-interference performance of the adaptive antenna arrays is significantly enhanced. The numerical experiments are employed to validate the proposed approach.

Index Terms - Beam forming**,** null depth**,** SINR transformation matrix**,** ***v***irtual array**.**

I. INTRODUCTION

Generally speaking, the number of interference signals processed by an antenna array should be less than the degrees of system freedom [1, 2]. In the practical applications, the size and number of array elements are finite; however, frequently the number of interferers is much larger than the number of array elements. Obviously, some of the interferers will not be effectively inhibited when the number of interferers exceeds the degrees of system freedom. Friedlander [3] has proposed a virtual array transformation (VAT) method that the number of virtual array elements can be increased to be more than the degrees of system freedom so that all the interferers can be processed.

When Friedlander's method is used in the beam forming of an adaptive antenna array, the null depth is relatively shallow compared to the real antenna array. Consequently, the output signal to interference and noise ratio (SINR) will be decreased; in turn, it is not suitable for the applications that require the higher communication quality. The existing improvement techniques with regarding to the VAT performance [4-6] are concentrated on the applications in the estimation of interference arriving direction. Shubair *et al*. combined the least mean mixed norm (LMMN) algorithm and initialization using sample matrix inversion (SMI) to control the error norms and offer the extra degrees of freedom [7]. In order to achieve the better virtual array performance, the influence generated by the transformation area selection on the beam forming is analyzed in the literature [8]. The literature [9] proposed a method to transform an arbitrary shaped array into a virtual uniform linear array (ULA) and then suppress multiple coherent interferences through the spatial smoothing technique.

Based on the conventional VAT beam forming algorithm, an improved VAT method is presented in this paper, which can be effectively applied to raise the inhibition gain by improving the null depth. By projecting the transformation matrix on the interference space that enhances the interference components in the virtual covariance matrix, a higher interference inhibition gain can be achieved.

II. VIRTUAL ARRAY TRANSFORMATION THEORY

Considering an array with N elements [10], when M far field narrow band signals are incident on an antenna array, the received data $\mathbf{X}$ can be expressed as follows:

$$\mathbf{X} = \mathbf{A}\mathrm{S}(t) + \mathbf{N}(t), \quad (1)$$

where $\mathbf{S}(t) = [s_1(t), s_2(t), \cdots, s_M(t)]^T$ is a vector containing the complex signal envelops of M narrow-band signal sources. $(\bullet)^T$ denotes the matrix transposition. $\mathbf{N}(t) = [n_1(t), n_2(t), \cdots, n_N(t)]^T$ is a vector of zero-mean spatially white sensor noise of variance σ_n^2. $\mathbf{A} = [\mathbf{a}(\theta_1), \mathbf{a}(\theta_2), \cdots \mathbf{a}(\theta_M)]$ is an array manifold vector, where $\mathbf{a}(\theta_k), (k = 1, 2 \cdots, M)$ represents a steering vector in the θ_k direction.

If an antenna array with N elements is uniform and linear, we have:

$$\mathbf{a}(\theta_k) = [1, e^{-j\frac{2\pi d}{\lambda}\sin\theta_k}, \cdots, e^{-j(N-1)\frac{2\pi d}{\lambda}\sin\theta_k}]^T, \quad (2)$$

where d is the space between two adjacent elements. If both the signal and noise are linearly independent, the data covariance can be represented as:

$$\mathbf{R} = E\left\{\mathbf{X}(t)\mathbf{X}^H(t)\right\} = \mathbf{A}\mathbf{R}_s\mathbf{A}^H + \sigma_n^2\mathbf{I}, \quad (3)$$

where $E(\bullet)$ denotes the mathematical expectation. $\mathbf{R}_s = E\left\{\mathrm{S}(t)\mathrm{S}^H(t)\right\}$ represents the autocorrelation matrix of signal complex envelops. σ_n^2 is the noise power. $\mathbf{I}$ is the unit matrix, and $(\bullet)^H$ denotes the matrix conjugate transposition. The array covariance matrix is estimated using the finite snap data $\mathbf{X}(i)$:

$$\hat{\mathbf{R}} = \frac{1}{K}\sum_{i=1}^{K}\mathbf{X}(i)\mathbf{X}^H(i),$$

where K is the snap number. In the array interpolation operation, the real array manifold is transformed on a preliminary specified virtual array manifold over a given angular sector Θ, namely, an interpolation matrix $\mathbf{B}$ is designed to satisfy:

$$\mathbf{B}\mathbf{a}(\theta) \approx \bar{\mathbf{a}}(\theta), \forall\theta \in \Theta, \quad (4)$$

where $\mathbf{a}(\theta)$ and $\bar{\mathbf{a}}(\theta)$ are $N \times 1$ and $\bar{N} \times 1$ steering vectors of the real and virtual arrays, respectively; $\bar{N}$ is the number of virtual elements; virtual array manifold $\bar{\mathbf{a}}(\theta)$ corresponds to a uniform linear array (ULA).

The computation of interpolation matrix $\mathbf{B}$ is carried out by choosing k representative directions $\theta_1, \theta_2, \cdots, \theta_k$ from the interpolation sector Θ, and minimizing the sum of quadratic interpolation errors in these directions:

$$F(\mathbf{B}) = \sum_{i=1}^{k}\left\|\mathbf{B}\mathbf{a}(\theta_i) - \bar{\mathbf{a}}(\theta_i)\right\|^2 = \left\|\mathbf{B}\mathbf{A} - \bar{\mathbf{A}}\right\|_F, \quad (5)$$

where $\mathbf{A}$ and $\bar{\mathbf{A}}$ are the real and virtual array manifold vector matrixes, respectively; and $\| \ \|_F$ denotes the *Frobenius* mold. The optimal minimum variance obtained from (5) is:

$$\mathbf{B} = \bar{\mathbf{A}}\mathbf{A}^H(\mathbf{A}\mathbf{A}^H)^{-1}. \quad (6)$$

After transformation, the covariance of virtual array becomes:

$$\bar{\mathbf{R}} = \mathbf{B}\mathbf{R}\mathbf{B}^H. \quad (7)$$

Through the noise-prewhitening process [3], the optimal weight can be obtained by using the minimum variance distortionless response method:

$$\mathbf{W}_{opt} = \alpha\bar{\mathbf{R}}^{-1}\bar{\mathbf{a}}(\theta_0), \quad (8)$$

where $\bar{\mathbf{a}}(\theta_0)$ represents a virtual array steering vector in the desired signal direction; and the coefficient $\alpha = \left[\bar{\mathbf{a}}^H(\theta_0)\bar{\mathbf{R}}^{-1}\bar{\mathbf{a}}(\theta_0)\right]^{-1}$.

III. NULL DEEPENING TECHNIQUE

Compared to the real array with the same parameters, the null depth formed by a virtual array in the Friedlander's VAT method is relatively shallow. To improve the null depth, we project the transformation matrix $\mathbf{B}$ on the interference space, and thus, the constraint information of the interference direction can be imported into the transformation matrix to enhance the interference components in the sampling covariance matrix. The detailed procedure is described as follows:

If the interference directions are $\theta_1, \theta_2, \cdots, \theta_{M'}$ and the number of interferers is M', the virtual array steering vector in the interferer directions $\bar{\mathbf{a}}(\theta_1), \bar{\mathbf{a}}(\theta_2), \cdots, \bar{\mathbf{a}}(\theta_{M'})$ can be calculated. Define a projection matrix $\mathbf{C}$ as:

$$\mathbf{C} = \left(\sum_{i=1}^{M'}\bar{\mathbf{a}}(\theta_i)\bar{\mathbf{a}}^H(\theta_i)\right)^H. \quad (9)$$

Projecting the transformation matrix on the interference space, we have:

$$\bar{\mathbf{B}} = \mathbf{C}\mathbf{B}. \quad (10)$$

Now the covariance matrix of virtual array becomes:

$$\tilde{\bar{\mathbf{R}}} = \bar{\mathbf{B}}\mathbf{R}\bar{\mathbf{B}}^H = \mathbf{C}\mathbf{B}\mathbf{R}\mathbf{B}^H\mathbf{C}^H = \mathbf{C}\bar{\mathbf{R}}\mathbf{C}^H. \quad (11)$$

After the mathematical operations, the information of the interference direction has already been involved in the transformed virtual covariance matrix $\tilde{\bar{\mathbf{R}}}$, and the interference components is strengthened.

IV. THEORETICAL ANALYSIS

According to Schmidt's orthogonal subspace resolution theory, using the eigenvalue decomposition from (7) $\bar{\mathbf{R}}$ can be expressed as [11]:

$$\bar{\mathbf{R}} = \bar{\mathbf{U}}\bar{\mathbf{\Sigma}}\bar{\mathbf{U}}^H, \tag{12}$$

where $\bar{\mathbf{U}}$ is an eigenvector vector of covariance matrix $\bar{\mathbf{R}}$, the diagonal matrix $\bar{\mathbf{\Sigma}}$ constituted by the corresponding eigenvalues is:

$$\bar{\mathbf{\Sigma}} = \begin{bmatrix} \bar{\lambda}_1 & & & \\ & \bar{\lambda}_2 & & \\ & & \ddots & \\ & & & \bar{\lambda}_{\bar{N}} \end{bmatrix}. \tag{13}$$

If a virtual array with $\bar{N}$ elements is ULA, the steering directions can be written as:

$$\bar{\mathbf{a}}(\theta_i) = [1, e^{-j\frac{2\pi\bar{d}}{\lambda}\sin\theta_i}, \cdots, e^{-j(\bar{N}-1)\frac{2\pi\bar{d}}{\lambda}\sin\theta_i}]^T, \tag{14}$$

where $\bar{d}$ is the space between two adjacent elements. We have:

$$\bar{\mathbf{a}}(\theta_i)\bar{\mathbf{a}}^H(\theta_i) = \begin{bmatrix} 1 \\ e^{-j\frac{2\pi\bar{d}}{\lambda}\sin\theta_i} \\ \vdots \\ e^{-j(\bar{N}-1)\frac{2\pi\bar{d}}{\lambda}\sin\theta_i} \end{bmatrix} \cdot [1, e^{-j\frac{2\pi\bar{d}}{\lambda}\sin\theta_i}, \cdots, e^{-j(\bar{N}-1)\frac{2\pi\bar{d}}{\lambda}\sin\theta_i}].$$

$$= \begin{bmatrix} 1, & e^{-j\frac{2\pi\bar{d}}{\lambda}\sin\theta_i}, & \cdots, & e^{-j(\bar{N}-1)\frac{2\pi\bar{d}}{\lambda}\sin\theta_i} \\ e^{-j\frac{2\pi\bar{d}}{\lambda}\sin\theta_i}, & e^{-j\cdot 2\cdot\frac{2\pi\bar{d}}{\lambda}\sin\theta_i}, & \cdots, & e^{-j(\bar{N}-1+1)\frac{2\pi\bar{d}}{\lambda}\sin\theta_i} \\ \vdots & \vdots & \cdots & \vdots \\ e^{-j(\bar{N}-1)\frac{2\pi\bar{d}}{\lambda}\sin\theta_i}, & e^{-j(\bar{N}-1+1)\frac{2\pi\bar{d}}{\lambda}\sin\theta_i}, & \cdots, & e^{-j\cdot 2\cdot(\bar{N}-1)\frac{2\pi\bar{d}}{\lambda}\sin\theta_i} \end{bmatrix}. \tag{15}$$

Substitute (15) into (9), we can obtain the expression of projection matrix $\mathbf{C}$:

$$\mathbf{C} = \left(\sum_{i=1}^{M'} \bar{\mathbf{a}}(\theta_i)\bar{\mathbf{a}}^H(\theta_i)\right)^H = \left(\sum_{i=1}^{M'} \begin{bmatrix} 1, & e^{-j\frac{2\pi\bar{d}}{\lambda}\sin\theta_i}, & \cdots, & e^{-j(\bar{N}-1)\frac{2\pi\bar{d}}{\lambda}\sin\theta_i} \\ e^{-j\frac{2\pi\bar{d}}{\lambda}\sin\theta_i}, & e^{-j\cdot 2\cdot\frac{2\pi\bar{d}}{\lambda}\sin\theta_i}, & \cdots, & e^{-j(\bar{N}-1+1)\frac{2\pi\bar{d}}{\lambda}\sin\theta_i} \\ \vdots & \vdots & \cdots & \vdots \\ e^{-j(\bar{N}-1)\frac{2\pi\bar{d}}{\lambda}\sin\theta_i}, & e^{-j(\bar{N}-1+1)\frac{2\pi\bar{d}}{\lambda}\sin\theta_i}, & \cdots, & e^{-j\cdot 2\cdot(\bar{N}-1)\frac{2\pi\bar{d}}{\lambda}\sin\theta_i} \end{bmatrix}\right)^H. \tag{16}$$

Substitute (12) and (13) into (11), then we have:

$$\tilde{\bar{\mathbf{R}}} = \mathbf{C}\bar{\mathbf{R}}\mathbf{C}^H = \mathbf{C}\bullet\left(\bar{\mathbf{U}}\bar{\mathbf{\Sigma}}\bar{\mathbf{U}}^H\right)\bullet\mathbf{C}^H = \mathbf{C}\bullet\left(\bar{\mathbf{U}}\bullet\begin{bmatrix} \bar{\lambda}_1 & & & \\ & \bar{\lambda}_2 & & \\ & & \ddots & \\ & & & \bar{\lambda}_{\bar{N}} \end{bmatrix}\bullet\bar{\mathbf{U}}^H\right)\bullet\mathbf{C}^H. \tag{17}$$

Substitute $\mathbf{C}$ into (17), $\tilde{\bar{\mathbf{R}}}$ can be expressed as:

$$\tilde{\bar{\mathbf{R}}} = \left(\sum_{i=1}^{M'} \begin{bmatrix} 1 \ , & e^{-j\frac{2\pi\bar{d}}{\lambda}\sin\theta_i}, & \cdots, & e^{-j(\bar{N}-1)\frac{2\pi\bar{d}}{\lambda}\sin\theta_i} \\ e^{-j\frac{2\pi\bar{d}}{\lambda}\sin\theta_i} , & e^{-j\cdot 2\cdot\frac{2\pi\bar{d}}{\lambda}\sin\theta_i}, & \cdots, & e^{-j(\bar{N}-1+1)\frac{2\pi\bar{d}}{\lambda}\sin\theta_i} \\ \vdots & \vdots & \cdots & \vdots \\ e^{-j(\bar{N}-1)\frac{2\pi\bar{d}}{\lambda}\sin\theta_i}, & e^{-j(\bar{N}-1+1)\frac{2\pi\bar{d}}{\lambda}\sin\theta_i}, & \cdots, & e^{-j\cdot 2\cdot(\bar{N}-1)\frac{2\pi\bar{d}}{\lambda}\sin\theta_i} \end{bmatrix} \right)^H \bullet \left(\bar{\mathbf{U}} \bullet \begin{bmatrix} \bar{\lambda}_1 & & & \\ & \bar{\lambda}_2 & & \\ & & \ddots & \\ & & & \bar{\lambda}_{\bar{N}} \end{bmatrix} \bullet \bar{\mathbf{U}}^H \right) \bullet$$

$$\left(\sum_{i=1}^{M'} \begin{bmatrix} 1 \ , & e^{-j\frac{2\pi\bar{d}}{\lambda}\sin\theta_i}, & \cdots, & e^{-j(\bar{N}-1)\frac{2\pi\bar{d}}{\lambda}\sin\theta_i} \\ e^{-j\frac{2\pi\bar{d}}{\lambda}\sin\theta_i} , & e^{-j\cdot 2\cdot\frac{2\pi\bar{d}}{\lambda}\sin\theta_i}, & \cdots, & e^{-j(\bar{N}-1+1)\frac{2\pi\bar{d}}{\lambda}\sin\theta_i} \\ \vdots & \vdots & \cdots & \vdots \\ e^{-j(\bar{N}-1)\frac{2\pi\bar{d}}{\lambda}\sin\theta_i}, & e^{-j(\bar{N}-1+1)\frac{2\pi\bar{d}}{\lambda}\sin\theta_i}, & \cdots, & e^{-j\cdot 2\cdot(\bar{N}-1)\frac{2\pi\bar{d}}{\lambda}\sin\theta_i} \end{bmatrix} \right), \qquad (18)$$

(18) can be further simplified as:

$$\begin{aligned} \tilde{\bar{\mathbf{R}}} &= \tilde{\bar{\mathbf{U}}} \bullet \begin{pmatrix} M'^2 \cdot \bar{\lambda}_1 & & & \\ & \left(1 + e^{-j\cdot 2\cdot\frac{2\pi\bar{d}}{\lambda}\sin\theta_1} + \cdots + e^{-j\cdot 2\cdot\frac{2\pi\bar{d}}{\lambda}\sin\theta_{M'}}\right)^2 \cdot \bar{\lambda}_2 & & \\ & & \ddots & \\ & & & \left(1 + e^{-j\cdot 2\cdot(\bar{N}-1)\cdot\frac{2\pi\bar{d}}{\lambda}\sin\theta_1} + \cdots + e^{-j\cdot 2\cdot(\bar{N}-1)\cdot\frac{2\pi\bar{d}}{\lambda}\sin\theta_{M'}}\right)^2 \cdot \bar{\lambda}_{\bar{N}} \end{pmatrix} \bullet \tilde{\bar{\mathbf{U}}}^H, \\ &= \tilde{\bar{\mathbf{U}}} \bullet \tilde{\bar{\boldsymbol{\Sigma}}} \bullet \tilde{\bar{\mathbf{U}}}^H \\ &= \tilde{\bar{\mathbf{U}}} \bullet \begin{bmatrix} \tilde{\bar{\lambda}}_1 & & & \\ & \tilde{\bar{\lambda}}_2 & & \\ & & \ddots & \\ & & & \tilde{\bar{\lambda}}_N \end{bmatrix} \bullet \tilde{\bar{\mathbf{U}}}^H, \end{aligned} \qquad (19)$$

where $\tilde{\bar{\mathbf{U}}}$ is the eigenvector matrix corresponding to $\tilde{\bar{\mathbf{R}}}$, $\tilde{\bar{\boldsymbol{\Sigma}}} = \begin{bmatrix} \tilde{\bar{\lambda}}_1 & & & \\ & \tilde{\bar{\lambda}}_2 & & \\ & & \ddots & \\ & & & \tilde{\bar{\lambda}}_{\bar{N}} \end{bmatrix}$ is the diagonal matrix constituted by the eigenvalues of $\tilde{\bar{\mathbf{R}}}$. From (19) it is obviously observed:

$$\tilde{\bar{\lambda}}_i > \bar{\lambda}_i, i = 1, 2, \cdots, \bar{N}. \qquad (20)$$

The eigenvalues of the covariance matrix obtained by using the improved VAT algorithm are bigger than those obtained from the conventional VAT algorithm.

Next, we briefly introduce the minimum variance distortionless response (MVDR) beam forming method [12]. In the direction of the desired signal, the gain is constrained to be 1, and the array output power is ensured to be minimum, namely, the interference and noise will generate the minimum output power. Applied to the virtual array, the weight vector of the MVDR beam forming is the solution to the following problem:

$$\begin{aligned} \mathbf{W}_{MVDR} &= \underset{\mathbf{W}^H \bar{\mathbf{a}}(\theta_0)=1}{\arg} \min E\left[\left| \mathbf{W}^H \bar{\mathbf{X}}(k) \right|^2 \right] \\ &= \underset{\mathbf{W}^H \bar{\mathbf{a}}(\theta_0)=1}{\arg} \min \mathbf{W}^H \tilde{\bar{\mathbf{R}}} \mathbf{W}, \end{aligned} \qquad (21)$$

where the $\underset{\mathbf{W}^H \bar{\mathbf{a}}(\theta_0)=1}{\arg} \min [\ ]$ represents the optimal solution which can minimize the function value in $[\ ]$ and satisfy the equality $\mathbf{W}^H \bar{\mathbf{a}}(\theta_0) = 1$. The *arg* represents an inverse function. It can be solved using Lagrangian multiplier method:

$$\mathbf{W}_{MVDR} = \frac{\tilde{\overline{\mathbf{R}}}^{-1}\overline{\mathbf{a}}(\theta_0)}{\overline{\mathbf{a}}^H(\theta_0)\tilde{\overline{\mathbf{R}}}^{-1}\overline{\mathbf{a}}(\theta_0)},$$

which is equivalent to (8). The characteristic of the MVDR method in the desired signal direction is that the gain is restrained to be 1 and the simultaneously array output power is ensured to be minimum. The higher the interference power in array is, the stronger it's inhibited in these directions. By introducing the constraint information of the interference direction into the transformation matrix **B** in the improved VAT algorithm, the new eigenvalues of the covariance matrix become bigger, and the signal components corresponding to them are strengthened. Therefore, in these directions the inhibition gains will increase by the the MVDR method, namely, the null depths will be deeper as showed in the beam pattern.

V. SIMULATION VERIFICATION

The original array with 5 elements is uniform and linear, and the element space is λ. The expected signal illumines from the 0° direction. The signal to noise ratio is *SNR*=0dB. Three independent interferers come from -60°, -40°, and 50° directions, respectively. The signal to interference ratio is $SIR = -40dB$. The virtual array with 8 elements is uniform and linear, and the element space is $\lambda/2$. The virtual transformation area is [-65°, 55°]. The step-size is 0.1°. The number of snapshots is 200. Figure 1 shows the gain comparison obtained by using the MVDR beam forming through the real array method, the conventional and improved VAT algorithms. Figure 2 shows the eigenvalue comparison of covariance matrix obtained using three methods. Figure 3 shows the comparison of output SINR obtained by three methods.

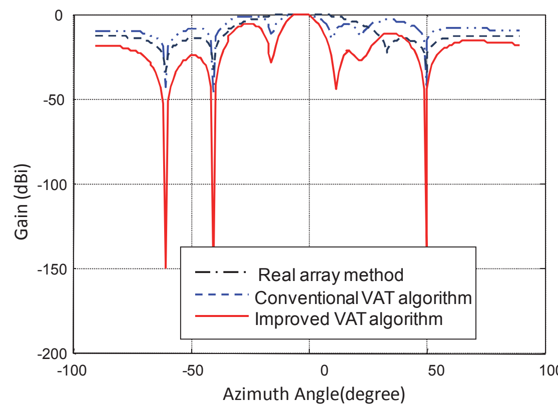

Fig. 1. Beam patterns using the different methods.

It is observed from Figures 1 to 3 that when the number of independent interferers is not larger than the number of the array elements, the nulls of the beam forming using the real array, conventional VAT, and the improved VAT algorithm are generated precisely in the interferer directions, and the main lobe is pointed to the desired signal direction. The inhibition gain using the real array and conventional VAT algorithms is about -35 dBi and -45 dBi, respectively. However, the inhibition gain using the proposed algorithm can reach up to -150 dBi. The eigenvalue of the covariance matrix has been significantly improved in the proposed method. Similarly, the output SINR has been significantly improved as well in the proposed method.

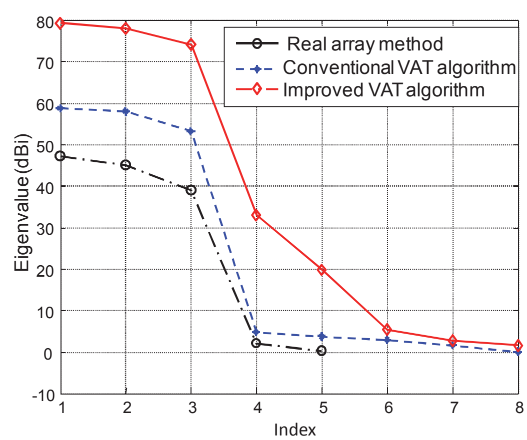

Fig. 2. Eigenvalues of the covariance matrix in the different methods.

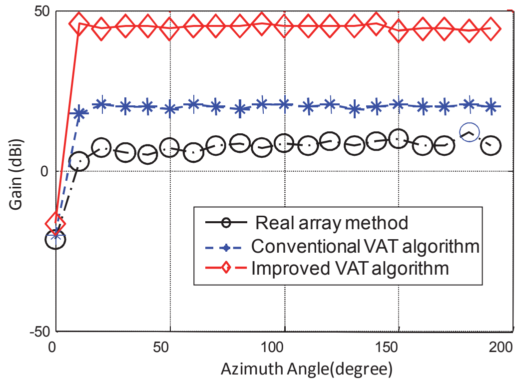

Fig. 3. Output SINR using the different methods.

Next, we use an example to validate the proposed method, in which the original array with 5 elements and space λ between the adjacent elements is uniform and linear. The desired signal incidence comes in the 0° direction. The signal to noise ratio is $SNR = 0dB$ and five independent interferers come in -60°, -40°, 20°, 50°, and 70° directions, respectively. The signal to interference ratio is $SIR = -40dB$. The virtual array with 8 elements and space $\lambda / 2$ between the adjacent elements is uniform and linear. The virtual transformation area is [-65°, 75°] and the step size is 0.1°. The number of snapshots is 200. Figure 4 shows the comparison of the MVDR beam forming using the different methods. Figure 5 shows the eigenvalue comparison of the covariance matrix using the three methods. Figure 6 shows the comparison of output SINR using three methods.

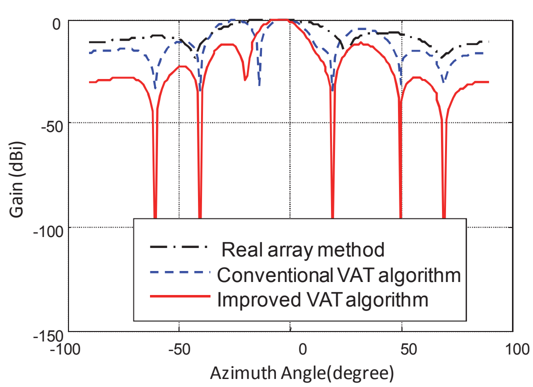

Fig. 4. Beam forming of five independent interferers using the different methods.

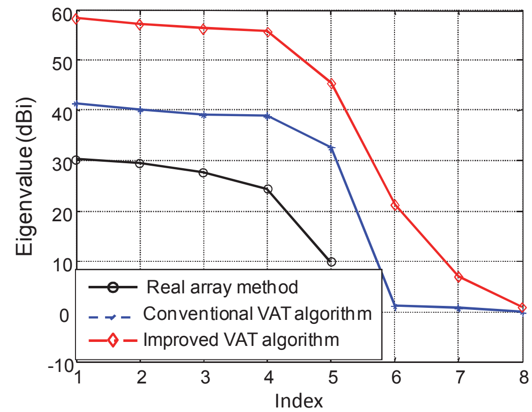

Fig. 5. Eigenvalues of five independent interferers using the different methods.

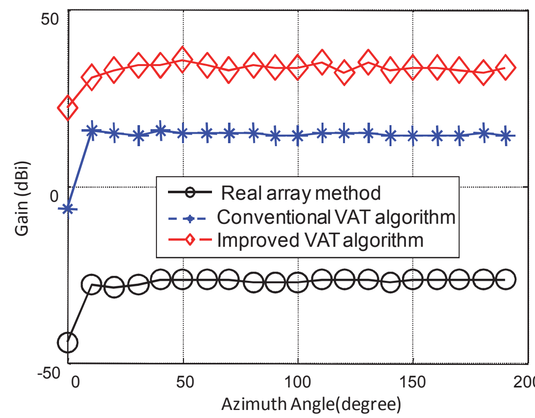

Fig. 6. Output SINR of five independent interferers using the different methods.

It is observed from Figs. 4 to 6 that when the number of interferers exceeds the freedom of original array, the nulls in the real array method cannot be generated in these interference directions. The virtual array with 8 elements cannot process all the interferers, but the nulls precisely point to these interferers. The inhibition gain using the conventional and proposed VAT algorithms is about -30 dB -120 dB, respectively. The eigenvalue of the improved algorithm has significantly improved, as well as the SINR.

VI. CONCLUSIONS

An improved VAT method has been presented in this paper, compared with the conventional approach; the null performance of beam forming is significantly improved. The nulls pointing to interference directions can be more steadily generated, and interference inhibition gains are much better and ensure a higher output SINR. Compared to the conventional algorithm, the proposed method only needs one more matrix multiplication operation.

REFERENCES

[1] M. Zatman, "Degree of Freedom Architectures for Large Adaptive Arrays," *Conference Record of the Asilomar Conference on Signals, Systems and Computers*, vol. 1, pp. 109-112, 1999.

[2] R. Games and R. Williams, "Performance Analysis of a Concurrent Adaptive Least-Squares Sidelobe Cancellation System with Excess Degrees of Freedom," *IEEE APS Int Symp Dig*., vol. 1, pp. 86-89, 1991.

[3] B. Friedlander, "The Root-Music Algorithm for Direction Finding with Interpolated Arrays," *Signal Processing*, vol. 30, no. 1, pp. 15-29, 1993.

[4] P. Hyberg, M. Jansson, and B. Ottersten, "Array Interpolation and Bias Reduction," *Signal Processing*, vol. 52, no. 10, pp. 2711-2720, 2004.

[5] M. Gavish and A. Weiss, "Direction Finding Using Esprit with Interpolated Arrays," *IEEE transactions on Signal Processing*, vol. 39, no. 6, pp. 1473-1478, 1991.

[6] M. Pesavento, A. Gershman, and Z. Luo. "Robust Array Interpolation Using Second Order Cone Programming," *IEEE Signal Processing Lett*, vol. 9, no. 1, pp. 8-11, 2002.

[7] R. Shubair, S. Jimaa, and A. Omar, "Robust Adaptive Beamforming Using Least Mean Mixed Norm Algorithm," *Applied Computational Electromagnetic Society (ACES) Journal*, vol. 23, no. 3, pp. 262-269, 2008.

[8] S. Baowei, "Robust Adaptive Beam Forming Via Array Transformation," *IEEE AP-S International Symposium on Antennas and Propagation*, DC, USA, vol. 1B, pp. 331-334, 2005.

[9] T. Lee and T. Lin, "Adaptive Beam Forming with Interpolated Arrays for Multiple Coherent Interferers," *Signal Processing*, vol. 57, no. 2, pp. 177-194, 1997.

[10] K. Reddy and V. Reddy, "Analysis of Interpolated Arrays with Spatial Smoothing," *Signal Processing*, vol. 54, no. 3, pp. 261-272, 1996.

[11] R. Schmidt, "Multiple Emitter Location and Signal Parameter Estimation," *IEEE Trans on Antennas and propagation*, vol. 34, no. 3, pp. 276-280, 1986.

[12] M. Souden and J. Benesty, "A Study of the LCMV and MVDR Noise Reduction Filters," *IEEE Transactions on Signal Processing*, vol. 58, no. 3, pp. 4925-4935, 2010.